Biosensors and Bioelectronics 42 (2013) 314–320

Contents lists available at SciVerse ScienceDirect

Biosensors and Bioelectronics

journal homepage: www.elsevier.com/locate/bios

Digital microfluidics with impedance sensing for integrated cell culture and analysis

Steve C.C. Shih [a,b], Irena Barbulovic-Nad [a,b], Xuning Yang [c], Ryan Fobel [a,b], Aaron R. Wheeler [a,b,d,*]

[a] Institute for Biomaterials and Biomedical Engineering, University of Toronto, 164 College St., Toronto, ON, Canada M5S 3G9
[b] Donnelly Centre for Cellular and Biomolecular Research, 160 College St., Toronto, Canada ON, M5S 3E1
[c] Department of Engineering Science, University of Toronto, 35 St George St., Toronto, ON, Canada M5S 1A4
[d] Department of Chemistry, University of Toronto, 80 St George St., Toronto, ON, Canada M5S 3H6

ARTICLE INFO

Article history:
Received 25 August 2012
Received in revised form
2 October 2012
Accepted 8 October 2012
Available online 26 October 2012

Keywords:
Digital microfluidics
Cell impedance
Multiplexing
Adherent cells
Electrowetting

ABSTRACT

We report the first digital microfluidic (DMF) system capable of impedance sensing of mammalian cells. The new system was validated in three assays: calibration, proliferation, and serum sensing. In the first assay, three cell lines (HeLa, CHO-K1, and NIH-3T3) were seeded at different densities to determine the relationship between impedance and cell number, which was found to be linear for each type of cell. In the proliferation assay, cells were grown for four days and their proliferation rates were determined by regular impedance measurements. In the serum sensing assay, a dilution series of cell media containing different concentrations of serum was evaluated using impedance measurements to determine the optimum conditions for proliferation. The DMF impedance system is label-free, does not require imaging, and is compatible with long-term cell culture. We propose that this system will be useful for the growing number of scientists who are seeking methods other than fluorescence or cell sorting to analyze adherent cells in situ.

1. Introduction

The most common techniques for studying cell populations are flow cytometry (Boeck, 2001; Dive et al., 1992) and fluorescence microscopy (Lippincott-Schwartz, 2011; Weinlich et al., 1998). Flow cytometry is particularly powerful as it affords the ability to rapidly evaluate large numbers of cells at the single-cell level. But flow cytometry is limited as the cells must be in suspension for analysis, which often requires enzymatic stripping of adherent cells from the surface they are cultured on. Fluorescence microscopy is thus a useful alternative, as it facilitates the evaluation of adherent cells in situ. But analysis by microscopy also causes significant perturbation through the loading of high concentrations of fluorescent dyes, and (in many cases) through the toxic processes of permeabilization and fixation.

An alternative to flow cytometry and fluorescence microscopy for analyzing the behavior of adherent cells is impedance analysis (Giaever and Keese, 1991, 1993; Holmes et al., 2009; Lo et al., 1995; Sun et al., 2010; Tiruppathi et al., 1992; Wegener et al., 1996). In this method, a layer of cells is grown on the surface of a micropatterned electrode and is exposed to low-magnitude AC voltage. Current then (a) flows between the cells such that the impedance is correlated with cell number, and (b) capacitatively couples through the cells such that the impedance is correlated with cell type and state. This method is growing in popularity, as it enables real-time analysis of cells in culture without the need for enzymatic stripping, fluorescent dyes, fixatives, or other perturbations (Keese et al., 2002, 2004). Variations of cell impedance analysis include using modified electrode surfaces patterned with self-assembled monolayers, antibodies, or carbon nanotubes (Abdolahad et al., 2012; Asphahani et al., 2008; Cheng et al., 2007; Mishra et al., 2005; Thein et al., 2010; Wang et al., 2008), and the use of varying electrode geometries (Brischwein et al., 2006; Rumenapp et al., 2009). A limitation for most cell impedance measurement systems relative to flow cytometry and microscopy is throughput. Typically, cell impedance analysis systems are integrated in multiwell plate format—e.g., the Applied Biophysics ECIS® system (http://www.biophysics.com). In laboratories lacking robotic dispensers and aspirators, this forms a practical limit to the throughput that is possible. Moreover, such techniques require significant cell and reagent use, making them cost-prohibitive for many researchers.

Microfluidics represents a potential solution to the multiplexing and reagent/cell use limitations of the multiwell plate format for impedance analysis. Most work in this area has focused on evaluating cells in suspension (Adams et al., 2008; Ayliffe and Frazier, 1999; Dharmasiri et al., 2009, 2011; Gawad et al., 2004; Sohn et al., 2000; Sun et al., 2009), or for forming traps to evaluate

* Corresponding author at: University of Toronto, Institute for Biomaterials and Biomedical Engineering, 164 College St., Toronto, ON, Canada M5S 3G9. Tel.: +1 416 946 3864; fax: +1 416 946 3865.
E-mail address: aaron.wheeler@utoronto.ca (A.R. Wheeler).

0956-5663/$ - see front matter © 2012 Elsevier B.V. All rights reserved.
http://dx.doi.org/10.1016/j.bios.2012.10.035

individual cells (Chen et al., 2011; Cho et al., 2006; Han and Frazier, 2006; Han et al., 2007, 2006; James et al., 2008; Jang and Wang, 2007). These techniques allow for significant savings in reagent and cell use; however, they are not compatible with analysis of adherent cells in situ. We are aware of only two reports of microfluidic systems used to evaluate adherent cells grown on the surface of electrodes (Curtis et al., 2009; DePaola et al., 2001). These papers represent an important first step for the goal of microfluidic cell impedance analysis, but the methods are not multiplexed. More work is needed to realize microfluidic cell impedance measurement systems capable of evaluating multiple experimental conditions in parallel.

Here, we report a new approach to integrating cell impedance analysis with microfluidics, relying on an alternative to microchannels for miniaturized analysis, digital microfluidics (DMF). In DMF, discrete droplets are manipulated by applying electrical fields to an array of electrodes (Abdelgawad and Wheeler, 2009; Wheeler, 2008), and the technique has recently become popular for the culture and analysis of suspension (Barbulovic-Nad et al., 2008; Fan et al., 2008; Shah et al., 2009, 2010) and adherent (Barbulovic-Nad et al., 2010; Bogojevic et al., 2012; Eydelnant et al., 2012; Srigunapalan et al., 2012; Vergauwe et al., 2011; Witters et al., 2011) cells, as well as cells grown as 3D constructs in gels (Fiddes et al., 2012). In all such systems reported previously, cells were monitored by fluorescence and/or microscopy. Here, we report the first combination of DMF with impedance sensing of cells, in a system capable of cell seeding, long-term culture, and multiplexed analysis. We propose that variations of this system may be useful for the growing number of scientists who are moving toward using impedance sensing to evaluate adherent cell behavior in situ.

2. Methods and materials

DMF device fabrication and operation, droplet operations and programs (i.e., S1–S3, C1–C2, E1–E3, and D1–D9), and the cell impedance circuit model are described in the online supplementary information.

2.1. Reagents and materials

Unless specified, general-use reagents were purchased from Sigma Chemical (Oakville, ON, Canada) or Fisher Scientific Canada (Ottawa, ON, Canada), and cell media and reagents were from Life Technologies (Burlington, ON, Canada). Deionized (DI) water had a resistivity of $\sim$18 MΩ cm at 25 °C, and was filtered through nylon syringe filters from Millipore (Billerica, MA, 0.2 μm pore diameter).

2.2. Macro-scale cell culture

HeLa, NIH-3T3, and CHO-K1 cells were grown in complete cell culture media formed from DMEM (HeLa and NIH-3T3) or 50/50 v/v F-12/DMEM (CHO-K1), supplemented with 10% fetal calf serum (FCS), penicillin (100 IU/mL) and streptomycin (100 μg/mL). Cells were grown to near confluency in complete media in T-25 flasks in an incubator at 37 °C with 5% CO_2. Prior to each DMF experiment, cells were detached using a solution of trypsin (0.25% w/v) and EDTA (1 mM), centrifuged, then resuspended in complete media supplemented with 0.05% Pluronic F68 (w/v) at the appropriate density.

2.3. Initial DMF cell impedance measurements

NIH-3T3 cells at two densities (0.5 and 2×10^6 cells/mL) were seeded (S1–S3) and cultured (C1–C2) in virtual microwells for 24 h. An image of each cell culture site was captured using a camera mated to a DM2000 upright microscope (Leica Microsystems Canada, Richmond Hill, ON, Canada). ImageJ software (Abramoff et al., 2004) was used to count the number of cells (N_c) and calculate the area occupied by the cells (A_c), which were $N_c = 60 \pm 6.2$ cells ($A_c = 2.55 \times 10^{-2}$ mm^2), and $N_c = 177 \pm 11.0$ cells, ($A_c = 1.34 \times 10^{-1}$ mm^2) for the low and high cell densities, respectively. V_{sense} was measured by applying a 1 s pulse of 100 V_{RMS} potential to the cell-sensor electrode relative to the top-plate electrode at frequencies of 5, 15, or 30 kHz. In a second experiment, after step C2, the culture media was exchanged (E1–E3) with aqueous sucrose (500 mM in DI water with 10 mM HEPES, 0.05% w/v Pluronic F68, pH 7.4) immediately prior to measurement of V_{sense} using the same parameters as above. Each condition was replicated five times, and paired t-tests were used to evaluate statistical significance.

2.4. DMF cell impedance assays

In calibration assays, suspensions of HeLa, NIH-3T3, and CHO-K1 cells at different volumetric densities (0.5, 1, and 2×10^6 cells/mL) were seeded (S1–S3), cultured (C1–C2) for 24 h the solution was exchanged with aqueous sucrose (E1–E3), and V_{sense} was measured at 15 kHz. Each condition was replicated five times and image-based cell surface densities and areas occupied by cells were calculated as above. Lines of regression were generated to relate V_{sense} to cell surface density.

In proliferation assays, suspensions of HeLa, NIH-3T3, and CHO-K1 cells at a volumetric density of 0.25×10^6 cells/mL were seeded (S1–S3), cultured (C1–C2) for 24 h, and exchanged with aqueous sucrose (E1–E3). V_{sense} at 15 kHz was measured and translated to a cell surface density using regression curves generated in the calibration assay. The sucrose solution was then exchanged with cell media (E1–E3) and then the cells were cultured (C1–C2) for 24 h. This process (E1–E3 with aqueous sucrose, measurement of V_{sense}, E1–E3 with fresh media, and C1–C2 for 24 h) was repeated after 48, 72, and 96 h. Each condition was replicated five times.

In serum screening assays, NIH-3T3 cells in complete media at a volumetric density of 0.25×10^5 cells/mL were seeded (S1–S3) and cultured (C1–C2) for 6 h. A dilution and exchange program was then executed to generate droplets containing five different concentrations of FCS (0.63%, 1.25%, 2.5%, 5%, and 10%) in media using DMEM fortified with 100 IU/mL penicillin, 100 μg/mL streptomycin, 0.05% w/v Pluronic F-68, and 20% FCS as "reagent", and the same solution without FCS as "diluent" for steps (D1–D9). Cells in virtual microwells containing each of these serum concentrations were then cultured (C1–C2) for 24 h and then exchanged with aqueous sucrose (E1–E3). V_{sense} at 15 kHz was measured and this value was translated to a cell surface density using the regression curve from the calibration assay. Media containing different concentrations of serum were then re-generated and used to exchange the sucrose solutions in the virtual microwells (D1–D9) and the cells were cultured (C1–C2) for an additional 24 h. This process (E1–E3 with aqueous sucrose, measurement of V_{sense}, D1–D9 to generate and replace with fresh media with different FCS concentrations, and C1–C2 for 24 h) was repeated after 48 and 72 h, culminating with a final analysis (E1–E3 with aqueous sucrose and measurement of V_{sense}) after 96 h. Each condition was replicated five times.

3. Results and discussion

3.1. Digital microfluidic system

Digital microfluidics has recently become popular for the culture and analysis of adherent cells (Barbulovic-Nad et al., 2010; Bogojevic

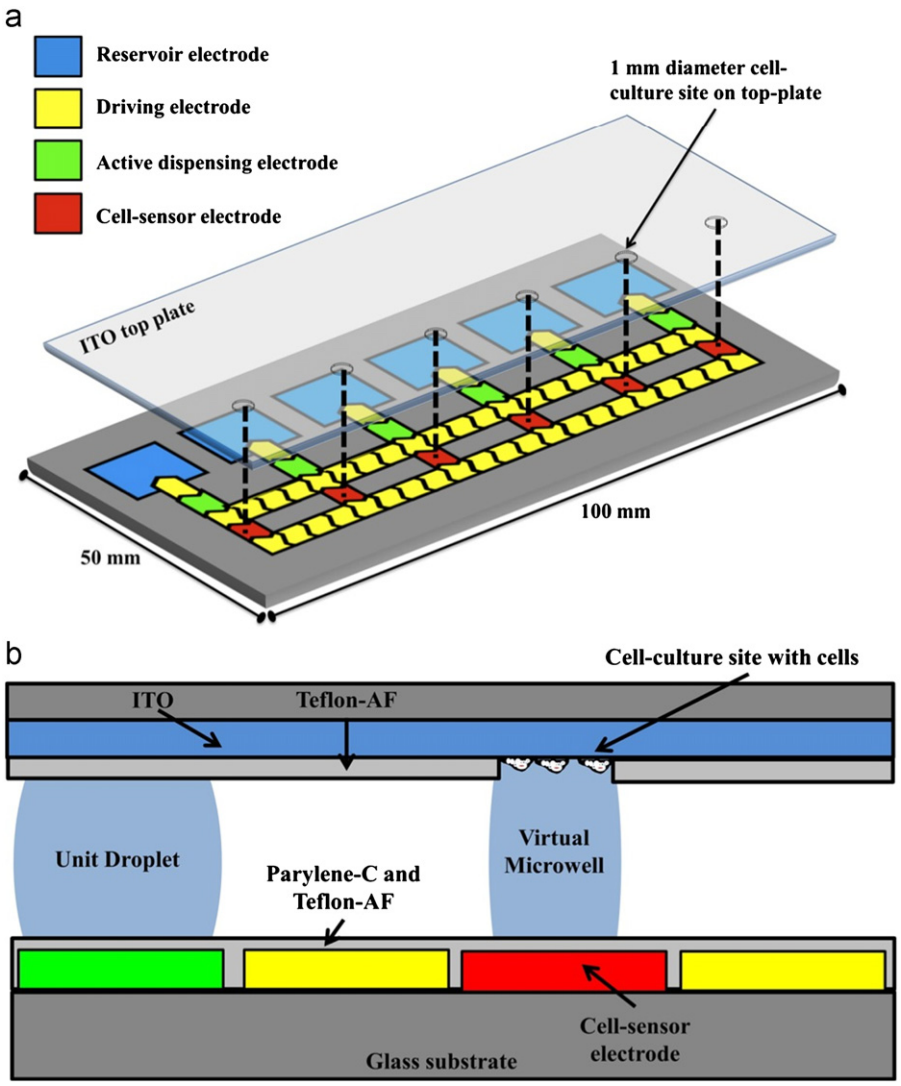

Fig. 1. Digital microfluidic device for cell culture and impedance sensing. (a) Top view of the device. The bottom plate bears 66 electrodes, and the top-plate has six patterned 1 mm dia. cell-culture sites (exposed ITO). (b) Side view of the DMF device. Unit droplets (~1 μL) cover the area over a single driving electrode. Virtual microwells (~0.2 μL) cover the area over a single cell culture site.

et al., 2012; Eydelnant et al., 2012; Srigunapalan et al., 2012; Vergauwe et al., 2011; Witters et al., 2011). In such systems, hydrophilic sites are patterned on the device surface to serve as sites for cell seeding, spreading, and proliferation. In addition to being useful for growing adherent cells, these hydrophilic sites also enable a fluidic phenomenon called passive dispensing, which occurs when a unit droplet (i.e., a droplet that covers the space over a single driving electrode) is translated across a hydrophilic site. This results in spontaneous formation of a sub-droplet known as a virtual microwell (Eydelnant et al., 2012). A unit droplet and a virtual microwell are featured in a schematic of the device used here, as shown in Fig. 1.

Fig. 2 depicts a typical process used for the work described here. As shown, a virtual microwell containing cells is formed (frames 1–2) followed by two reagent exchanges (frames 3–4 and 5–6). In practice, this process [represented by steps S1–S3 and E1–E3 (twice) from the online supplementary information] requires 104 droplet movements onto energized electrodes. A challenge for such complex programs, particularly for those in which the medium surrounding droplets is air (as in the work described here), is the phenomenon of imperfect droplet movement fidelity: droplets occasionally fail to move onto an energized destination electrode. To overcome this problem, we adopted a strategy in which impedance sensing is used to enable feedback control to improve the fidelity of droplet manipulation (Shih et al., 2011). The feedback control system used here is shown in Fig. S1 in the online supplementary information, which operates by repeatedly measuring a voltage (V_{sense}) that correlates with droplet impedance.

3.2. Cell impedance measurement system

We hypothesized that the impedance measurement system used for feedback control over droplet position (Fig. S1) could be repurposed to measure the impedance of adherent cells. To test this hypothesis, NIH-3T3 cells were seeded (as in Fig. 2, frames 1–2) at low and high densities (0.5 and 2×10^6 cells/mL) and were incubated for 24 h. V_{sense} values were then measured at three different frequencies, which are shown in Fig. 3a as discrete points for the low (green) and high (red) density cases. Unfortunately, the differences between these values were not statistically significant. For example, at 15 kHz, the V_{sense} values were 71.5 ± 4.9 mV and 78.3 ± 6.6 mV respectively ($p = 0.101$). This suggests that these conditions are not ideal for measuring cell density as a function of impedance.

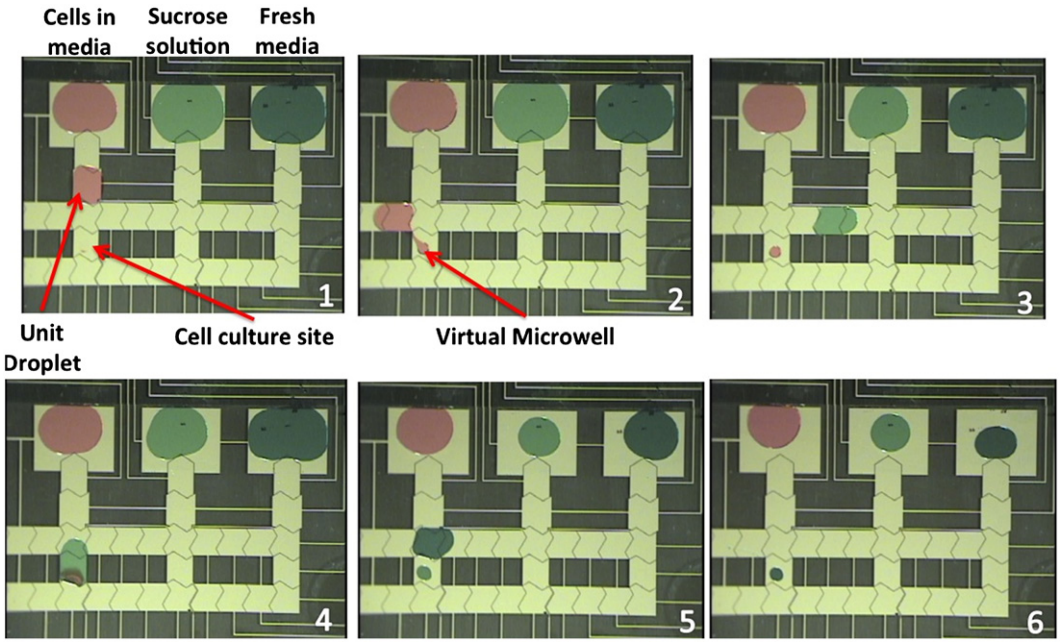

Fig. 2. Frames from a movie depicting a multistep experiment. In frames 1–2, a virtual microwell containing cells is formed. After incubation, in frames 3–4, the contents of the virtual microwell are exchanged with a sucrose suspension. Finally, in frames 5–6, the contents of the virtual microwell are exchanged with fresh media. Colored dye was added to aid in visualization.

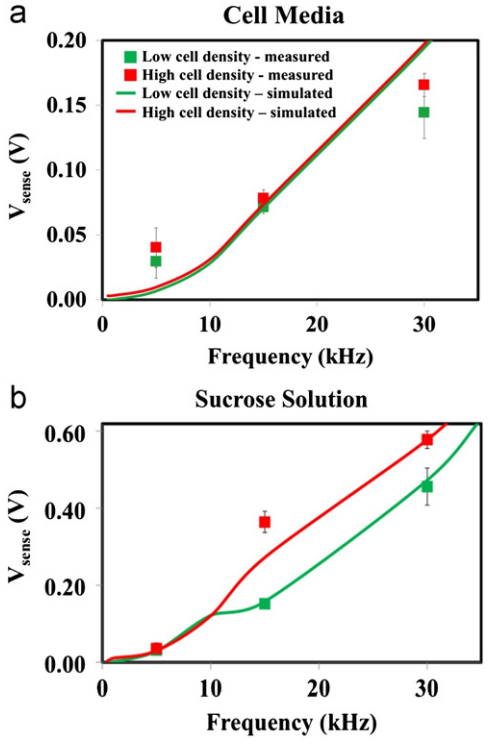

Fig. 3. Graphs of measured (solid squares; error bars represent ± 1 S.D.) and simulated (solid lines) V_{sense} values in (a) cell media and (b) 500 mM sucrose as a function of frequency. Green and red are indicators for volumetric cell densities of 0.5×10^6 and 2.0×10^6 cells/mL, respectively. Simulated V_{sense} values were generated using the circuit shown in Table S1 in the online supplementary information. In (a), the simulated curves have identical values; a slight artificial offset was added to the red curve to show that there are two curves. (For interpretation of the references to color in this figure legend, the reader is referred to the web version of this article.)

We hypothesized that the correlation between V_{sense} and cell density might be improved by using a buffered, isotonic medium with lower conductivity than cell media, a technique commonly used in dielectrophoresis applications (Gray et al., 2004; Taff and Voldman, 2005). To test this hypothesis, the media in virtual microwells was exchanged with a low-conductivity sucrose solution (as in Fig. 2, frames 3–4) prior to measuring V_{sense}. These data, shown as discrete points in Fig. 3b, are promising. For example, for measurements at 15 kHz, the V_{sense} values for low and high densities were 151.2 ± 11.9 mV and 364.6 ± 27.4 mV. This difference is significant ($p = 2.36 \times 10^{-7}$), and confirms that low-conductivity liquids are favorable for impedance sensing of cells. Methods were developed to rapidly exchange the sucrose solution with fresh cell culture media (as in Fig. 2, frames 5–6) after the analysis. In typical experiments, this resulted in cells being exposed to the sucrose solution for $\sim$10 min, a condition which did not impact cell proliferation rates for any of the cell types evaluated here (data not shown).

To understand the experimental results described above, we developed a circuit model, shown in Table S1 in the online supplementary information. The circuit was adapted from those described previously (Morgan et al., 2007; Sun and Morgan, 2010; Sun et al., 2010), and includes a resistor and a capacitor in parallel to model the liquid medium (element 2 in Table S1) and capacitors and a resistor in series to model the cell membrane and cytoplasm respectively (the top sub-circuit of element 3 in Table S1). But the models used previously are not a perfect match to the experimental system used here. One key difference is the presence of the insulator covering the bottom-plate electrode of the DMF device; all other cell impedance measurement systems that we are aware of use bare electrodes that make direct contact with cells and media. We added a capacitor (element 1 in Table S1) to the model to account for this difference. A second difference is the fact that cells in the new system are adhered to the electrode, whereas the models used previously were designed for a system in which cells were not in contact with the electrodes. To accommodate this difference, we added a separate sub-circuit to model liquid at the interface between the droplet and the electrode (the bottom sub-circuit of element 3 in Table S1).

V_{sense} values predicted by the circuit model are plotted as solid lines in Fig. 3. Although the simulations are not a perfect match to

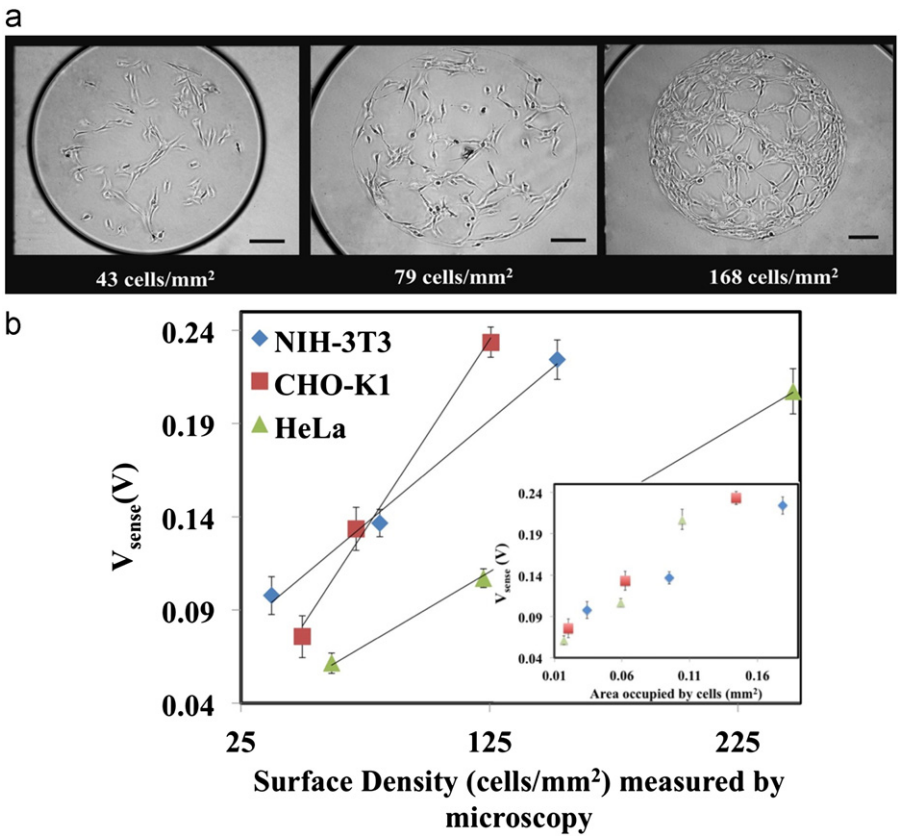

Fig. 4. Calibration assay. (a) Pictures showing NIH-3T3 cells seeded at three different volumetric densities (0.5×10^6, 1.0×10^6, and 2.0×10^6 cells/mL) in virtual microwells. Scale bars are 10 μm, and the surface densities are listed under each picture. (b) Plots of V_{sense} as a function of surface density for NIH-3T3 (blue diamonds), HeLa (green triangles), and CHO-K1 (red squares) cells. The inset shows the same data plotted as a function of the area occupied by the cells. Error bars represent ± 1 S.D. (For interpretation of the references to color in this figure legend, the reader is referred to the web version of this article.)

the experimental data, the key trends are reproduced, including accurate predictions that lower conductivity media and higher analysis frequencies are preferable for correlating impedance to cell density. There are a number of potential causes for the differences between the experimental and simulated data. One potential source of variation is changes in the effective area of the electrode observed as a function of changes in droplet contact angle. A second potential source of variation is imperfect estimation of area occupied by the cells in the model, and a third is imperfect estimation of cell membrane capacitance and cytoplasm resistance. Clearly, more work is required to generate a better model, but the accuracy in predicting the most important trends gives us confidence to understand the basic elements of the measurement.

3.3. DMF-cell impedance assays

To evaluate the utility of the cell impedance measurement system for DMF applications, we developed three assays: (1) calibration, (2) proliferation, and (3) serum screening. For the first assay, three cell lines (CHO-K1, NIH-3T3, and HeLa) were seeded in virtual microwells, cultured overnight, and then exchanged with sucrose solution. Images were used to calculate the resulting surface densities and areas occupied by the cells (Fig. 4a), and V_{sense} was then plotted as a function of cell surface density (Fig. 4b). The regression lines were linear (R^2=0.9920, 0.9935, 0.9965 for CHO-K1, NIH-3T3, and HeLa cells) over at least one order of magnitude (higher densities were not tested). The limits of detection (LOD) were ~20–25 cells/mm^2. The model (Table S1) suggests that in the future, the LOD might be lowered by using a thinner insulator, reduced spacing between top and bottom plate, and smaller electrode area. The apparent differences between cell lines can be partly explained by differences in cell area (Fig. 4b-inset); any remaining differences are likely a function of the known differences in capacitative coupling for different cell types (Giaever and Keese, 1991; Holmes et al., 2009).

In the second assay, three cell lines were seeded and cultured for four days and cell growth was monitored periodically using the methods described above. Fig. 5a shows growth curves for each cell line, in which V_{sense} values were translated to surface cell densities from the data in Fig. 4. As shown, on day 1, cell numbers were below the detection limits, but on each later day measurable values were obtained. The trend of NIH-3T3 and HeLa cells proliferating faster than CHO-K1 cells (highlighted in Fig. 5b) was identical to that observed for cells cultured in standard conditions (data not shown).

The third assay was motivated by the wide-spread interest in reducing the serum content in vitro cell culture (Ikeda et al., 1995; Mengual Gomez et al., 2010). NIH-3T3 cells were seeded and grown in a dilution series of fetal calf serum at different concentrations (generated on-chip) for four days, with periodic impedance measurements to evaluate cell density (Fig. 6a). As shown, at 5% and 10% serum, cell growth followed sigmoidal profiles, while at lower concentrations cells did not grow well. In the future, we propose that variations of this method might be useful for a wide range of other types of assays in which we use cell proliferation rate as the readout—e.g., drug screening (Kunas and Papoutsakis, 2009; Mengual Gomez et al., 2010; Otto et al., 2003; Stolwijk et al., 2011), gene expression (Zudaire et al., 2008), and wound-healing (Keese et al., 2004; Lundien et al., 2002).

As depicted in Fig. 6b, the method was carried out in 6-plex format, and we propose that it would be straightforward to expand

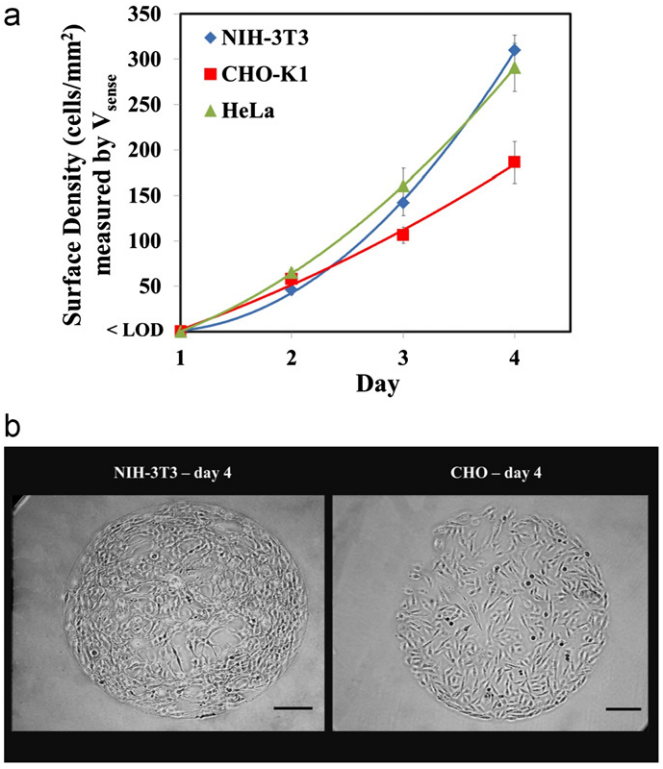

Fig. 5. Proliferation assay. (a) Graph of surface density measured by impedance as a function of time for NIH-3T3 (blue diamonds), CHO-K1 (red squares), and HeLa (green triangles) cultured for four days. Curves were added to guide the eye, and error bars represent ± 1 S.D. (b) Pictures of NIH-3T3 (left) and CHO-K1 (right) cells cultured in virtual microwells for four days confirming the differences in proliferation rates. Scale bars are 10 μm. (For interpretation of the references to color in this figure legend, the reader is referred to the web version of this article.)

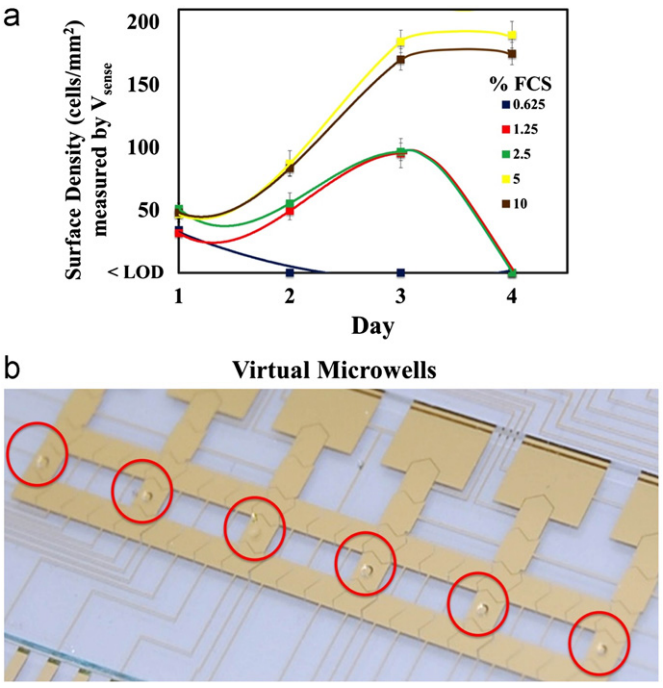

Fig. 6. Serum screening assay. (a) Growth curves for NIH-3T3 cells cultured in virtual microwells of media containing 0.63% (blue squares), 1.25% (red squares), 2.5% (green squares), 5% (yellow squares), and 10% (brown squares) fetal calf serum. Curves were added to guide the eye, and error bars represent ± 1 S.D. (b) Picture showing six virtual microwells containing cells on a device. (For interpretation of the references to color in this figure legend, the reader is referred to the web version of this article.)

this technique to higher levels of multiplexing, particularly with the recent report of DMF devices with 4096 independent electrodes (Hadwen et al., 2012). In addition, the method reported here enables nearly 1000-fold reduction in reagent-use compared to cell impedance analysis systems available commercially; e.g., the Applied Biophysics ECIS® system requires 1.5–4 mL per assay (Giaever and Keese, 1991; Tiruppathi et al., 1992), while corresponding assay requires 1–10 μL in the DMF format. Finally, DMF also enables media exchange without intervention, suggesting the possibility of uninterrupted culture and analysis for long periods of time. We propose that the new methods described here may be particularly useful for applications involving small numbers of precious cells and for assays involving frequent media/reagent exchange steps.

4. Conclusion

We have developed the first digital microfluidic method capable of cell impedance sensing. The new method incorporates a feedback control system enabling high-fidelity droplet movement without manual intervention, and enables impedance analyses with nearly 1000-fold reduction in reagent use relative to commercial alternatives. We anticipate this new method will be useful for the growing number of researchers seeking alternatives to flow cytometry and fluorescence microscopy for analyzing adherent cells in situ.

Acknowledgments

S.C.C.S., I.B.N., and R.F. thank the Natural Sciences and Engineering Research Council (NSERC) and the province of Ontario for fellowships. A.R.W. thanks the Canada Research Chair (CRC) program for a CRC. We thank NSERC and the Canadian Institutes of Health Research (CIHR) for research funding.

Appendix A. Supporting information

Supplementary data associated with this article can be found in the online version at doi:10.1016/j.bios.2012.10.035.

References

Abdelgawad, M., Wheeler, A.R., 2009. Advanced Materials 21, 920–925.
Abdolahad, M., Taghinejad, M., Taghinejad, H., Janmaleki, M., Mohajerzadeh, S., 2012. Lab on a Chip 12, 1183–1190.
Abramoff, M.D., Magalhaes, P.J., Ram, S.J., 2004. Biophotonics International 11, 36–42.
Adams, A.A., Okagbare, P.I., Feng, J., Hupert, M.L., Patterson, D., Gottert, J., McCarley, R.L., Nikitopoulos, D., Murphy, M.C., Soper, S.A., 2008. Journal of the American Chemical Society 130, 8633–8641.
Asphahani, F., Thein, M., Veiseh, O., Edmondson, D., Kosai, R., Veiseh, M., Xu, J., Zhang, M., 2008. Biosensors and Bioelectronics 23, 1307–1313.
Ayliffe, H.E., Frazier, A.B., 1999. Journal of Microelectromechanical Systems 8, 50–57.
Barbulovic-Nad, I., Au, S.H., Wheeler, A.R., 2010. Lab on a Chip 10, 1536–1542.
Barbulovic-Nad, I., Yang, H., Park, P.S., Wheeler, A.R., 2008. Lab on a Chip 8, 519–526.
Boeck, G., 2001. International Review of Cytology—a Survey of Cell Biology 204, 239–298.
Bogojevic, D., Chamberlain, M.D., Barbulovic-Nad, I., Wheeler, A.R., 2012. Lab on a Chip 12, 627–634.
Brischwein, M., Herrmann, S., Vonau, W., Berthold, F., Grothe, H., Motrescu, E.R., Wolf, B., 2006. Lab on a Chip 6, 819–822.
Chen, J., Zheng, Y., Tan, Q., Zhang, Y.L., Li, J., Geddie, W.R., Jewett, M.A., Sun, Y., 2011. Biomicrofluidics 5, 14113.
Cheng, X., Liu, Y.S., Irimia, D., Demirci, U., Yang, L., Zamir, L., Rodriguez, W.R., Toner, M., Bashir, R., 2007. Lab on a Chip 7, 746–755.

Cho, Y.H., Yamamoto, T., Sakai, Y., Fujii, T., Kim, B., 2006. Journal of Microelectromechanical Systems 15, 287–295.
Curtis, T.M., Widder, M.W., Brennan, L.M., Schwager, S.J., van der Schalie, W.H., Fey, J., Salazar, N., 2009. Lab on a Chip 9, 2176–2183.
DePaola, N., Phelps, J.E., Florez, L., Keese, C.R., Minnear, F.L., Giaever, I., Vincent, P., 2001. Annals of Biomedical Engineering 29, 648–656.
Dharmasiri, U., Balamurugan, S., Adams, A.A., Okagbare, P.I., Obubuafo, A., Soper, S.A., 2009. Electrophoresis 30, 3289–3300.
Dharmasiri, U., Njoroge, S.K., Witek, M.A., Adebiyi, M.G., Kamande, J.W., Hupert, M.L., Barany, F., Soper, S.A., 2011. Analytical Chemistry 83, 2301–2309.
Dive, C., Gregory, C.D., Phipps, D.J., Evans, D.L., Milner, A.E., Wyllie, A.H., 1992. Biochimica et Biophysica Acta 1133, 275–285.
Eydelnant, I.A., Uddayasankar, U., Li, B., Liao, M.W., Wheeler, A.R., 2012. Lab on a Chip 12, 750–757.
Fan, S.K., Huang, P.W., Wang, T.T., Peng, Y.H., 2008. Lab on a Chip 8, 1325–1331.
Fiddes, L.K., Luk, V.N., Au, S.H., Ng, A.H.C., Luk, V.M., Kumacheva, E., Wheeler, A.R., 2012. Biomicrofluidics 6, 014112.
Gawad, S., Cheung, K., Seger, U., Bertsch, A., Renaud, P., 2004. Lab on a Chip 4, 241–251.
Giaever, I., Keese, C.R., 1991. Proceedings of the National Academy of Sciences of the United States of America 88, 7896–7900.
Giaever, I., Keese, C.R., 1993. Nature 366, 591–592.
Gray, D.S., Tan, J.L., Voldman, J., Chen, C.S., 2004. Biosensors and Bioelectronics 19, 1765–1774.
Hadwen, B., Broder, G.R., Morganti, D., Jacobs, A., Brown, C., Hector, J.R., Kubota, Y., Morgan, H., 2012. Lab on a Chip 12, 3305–3313.
Han, A., Frazier, A.B., 2006. Lab on a Chip 6, 1412–1414.
Han, A., Yang, L., Frazier, A.B., 2007. Clinical Cancer Research 13, 139–143.
Han, K.H., Han, A., Frazier, A.B., 2006. Biosensors and Bioelectronics 21, 1907–1914.
Holmes, D., Pettigrew, D., Reccius, C.H., Gwyer, J.D., van Berkel, C., Holloway, J., Davies, D.E., Morgan, H., 2009. Lab on a Chip 9, 2881–2889.
Ikeda, M., Kohno, M., Takeda, T., 1995. Hypertension 26, 401–405.
James, C.D., Reuel, N., Lee, E.S., Davalos, R.V., Mani, S.S., Carroll-Portillo, A., Rebeil, R., Martino, A., Apblett, C.A., 2008. Biosensors and Bioelectronics 23, 845–851.
Jang, L.S., Wang, M.H., 2007. Biomedical Microdevices 9, 737–743.
Keese, C.R., Bhawe, K., Wegener, J., Giaever, I., 2002. Biotechniques 33, 842–844.
Keese, C.R., Wegener, J., Walker, S.R., Giaever, I., 2004. Proceedings of the National Academy of Sciences of the United States of America 101, 1554–1559.
Kunas, K.T., Papoutsakis, E.T., 2009. Biotechnology and Bioengineering 102, 980–987, discussion 977–989.
Lippincott-Schwartz, J., 2011. Annual Review of Biochemistry 80, 327–332.
Lo, C.M., Keese, C.R., Giaever, I., 1995. Biophysical Journal 69, 2800–2807.
Lundien, M.C., Mohammed, K.A., Nasreen, N., Tepper, R.S., Hardwick, J.A., Sanders, K.L., Van Horn, R.D., Antony, V.B., 2002. Journal of Clinical Immunology 22, 144–152.
Mengual Gomez, D.L., Belaich, M.N., Rodriguez, V.A., Ghiringhelli, P.D., 2010. BMC Biotechnology 10, 68.
Mishra, N.N., Retterer, S., Zieziulewicz, T.J., Isaacson, M., Szarowski, D., Mousseau, D.E., Lawrence, D.A., Turner, J.N., 2005. Biosensors and Bioelectronics 21, 696–704.
Morgan, H., Sun, T., Holmes, D., Gawad, S., Green, N.G., 2007. Journal of Physics D: Applied Physics 40, 61–70.
Otto, A.M., Brischwein, M., Niendorf, A., Henning, T., Motrescu, E., Wolf, B., 2003. Cancer Detection and Prevention 27, 291–296.
Rumenapp, C., Remm, M., Wolf, B., Gleich, B., 2009. Biosensors and Bioelectronics 24, 2915–2919.
Shah, G.J., Ohta, A.T., Chiou, E.P., Wu, M.C., Kim, C.J., 2009. Lab on a Chip 9, 1732–1739.
Shah, G.J., Veale, J.L., Korin, Y., Reed, E.F., Gritsch, H.A., Kim, C.J., 2010. Biomicrofluidics 4, 44106.
Shih, S.C.C., Fobel, R., Kumar, P., Wheeler, A.R., 2011. Lab on a Chip 11, 535–540.
Sohn, L.L., Saleh, O.A., Facer, G.R., Beavis, A.J., Allan, R.S., Notterman, D.A., 2000. Proceedings of the National Academy of Sciences of the United States of America 97, 10687–10690.
Srigunapalan, S., Eydelnant, I.A., Simmons, C.A., Wheeler, A.R., 2012. Lab on a Chip 12, 369–375.
Stolwijk, J.A., Hartmann, C., Balani, P., Albermann, S., Keese, C.R., Giaever, I., Wegener, J., 2011. Biosensors and Bioelectronics 26, 4720–4727.
Sun, T., Morgan, H., 2010. Microfluidics and Nanofluidics 8, 423–443.
Sun, T., Swindle, E.J., Collins, J.E., Holloway, J.A., Davies, D.E., Morgan, H., 2010. Lab on a Chip 10, 1611–1617.
Sun, T., van Berkel, C., Green, N.G., Morgan, H., 2009. Microfluidics and Nanofluidics 6, 179–187.
Taff, B.M., Voldman, J., 2005. Analytical Chemistry 77, 7976–7983.
Thein, M., Asphahani, F., Cheng, A., Buckmaster, R., Zhang, M., Xu, J., 2010. Biosensors and Bioelectronics 25, 1963–1969.
Tiruppathi, C., Malik, A.B., Del Vecchio, P.J., Keese, C.R., Giaever, I., 1992. Proceedings of the National Academy of Sciences of the United States of America 89, 7919–7923.
Vergauwe, N., Witters, D., Ceyssens, F., Vermeir, S., Verbruggen, B., Puers, R., Lammertyn, J., 2011. Journal of Micromechanics and Microengineering 21, 054026.
Wang, L., Zhu, J., Deng, C., Xing, W.L., Cheng, J., 2008. Lab on a Chip 8, 872–878.
Wegener, J., Sieber, M., Galla, H.J., 1996. Journal of Biochemical and Biophysical Methods 32, 151–170.
Weinlich, M., Heydasch, U., Mooren, F., Starlinger, M., 1998. Research in Experimental Medicine (Berl) 198, 73–82.
Wheeler, A.R., 2008. Science 322, 539–540.
Witters, D., Vergauwe, N., Vermeir, S., Ceyssens, F., Liekens, S., Puers, R., Lammertyn, J., 2011. Lab on a Chip 11, 2790–2794.
Zudaire, E., Cuesta, N., Murty, V., Woodson, K., Adams, L., Gonzalez, N., Martinez, A., Narayan, G., Kirsch, I., Franklin, W., Hirsch, F., Birrer, M., Cuttitta, F., 2008. Journal of Clinical Investigation 118, 640–650.